

https://doi.org/10.1070/QEL18065

Prospects for anisotropic superfluidity in a Fermi gas of dysprosium

V.A. Vinogradov, K.A. Karpov, M.V. Platonova, A.V. Turlapov

Abstract. **The possibility of obtaining superfluid phases for a Fermi gas of dysprosium with a magnetic dipole–dipole interaction is discussed. The obstacles and possible solutions are shown. The required phases are similar to the A1 phase and the polar β phase in ^{3}He. It is expected that in dysprosium, the macroscopic properties of the phase will be determined by the symmetry of the pair interactions. It is assumed to observe the kinetics of phase formation and spontaneous choice between two energy-degenerate phases with different projections of the orbital angular momentum.**

Keywords: *laser trapping and cooling, gas of atoms, superfluidity, anisotropy, dipole–dipole interaction.*

1. Introduction

A number of phase transitions are associated with the formation of Cooper pairs with a nonzero angular momentum: high-temperature superconductivity in cuprates is accompanied by pairing in the d-channel [1], while 18 phases with p-symmetry of the order parameter have been predicted for ^{3}He [2]. Phases with p-pairing are characterised by nontrivial topological properties [3, 4].

In experiments with ultracold gases of atoms, a number of new effects related to the s-interaction were observed. These effects include the stability of the Fermi matter with a resonantly strong s-attraction [5], the phase transition to superfluidity in a similar regime [6], the BCS–BEC crossover whcih is a smooth transformation of a gas of Cooper pairs, obeying the Bardeen–Cooper–Schrieffer model, into a Bose–Einstein condensate of dimer molecules [7, 8].

Phase transitions associated with p-interaction and interactions with a higher angular momentum have not yet been observed in the gas of atoms, for which there are several reasons. Firstly, phase transitions usually require a sufficiently low temperature in Fermi energy units E_F. For example, in cuprate superconductors $T_{cr} \approx 0.01E_F$ [9], while the lowest temperature reached in the Fermi gas of atoms, $T_{min} = 0.1E_F$, is an order of magnitude higher. A possible, not yet implemented way to reduce the T_{min}/E_F ratio is associated with an increase in the number of atoms at the last stage of cooling [10]. Secondly, the gases are extremely diluted, and the interparticle distance is 0.1–1 μm, which is 30–300 times greater than that in the air. In collisions with characteristic energies of 0.1–10 μK, particles with the angular momentum $l \geqslant 1$ do not penetrate beyond the centrifugal barrier into the molecular potential region and, therefore, do not experience the interaction. Enhancing the interaction by means of Fano–Feshbach resonances, for example in the p-channel, led to inelastic three-particle collisions accompanied by the formation of molecules, heating, and loss of particles from traps [11].

A possible way to obtain a gas with a sufficiently strong interaction in the p-, and maybe in the d-channel, is to use a gas of heavy magnetic atoms. The dysprosium atom has the largest magnetic moment $d = 10\mu_B$, where μ_B is the Bohr magneton. Quantum degeneration of the fermionic isotope of dysprosium was achieved in [12].

This paper discusses the possibility of achieving a superfluid phase with an anisotropic order parameter in a dysprosium gas, associated difficulties, and ways to resolve them. A comparison is made between the observed superfluidity of ^{3}He and the expected properties of the atomic system.

2. Magnetic dipole–dipole interactions

In general, the interaction potential of two magnetic dipoles has the form [13]

$$V(\boldsymbol{r}) = \frac{\boldsymbol{d}_1\boldsymbol{d}_2}{r^3} - \frac{3(\boldsymbol{d}_1\boldsymbol{r})(\boldsymbol{d}_2\boldsymbol{r})}{r^5} - \frac{8\pi}{3}\boldsymbol{d}_1\boldsymbol{d}_2\delta(\boldsymbol{r}), \quad (1)$$

where $\boldsymbol{d}_1$, $\boldsymbol{d}_2$ are the magnetic dipole moments of atoms; and $\boldsymbol{r}$ is a vector directed from one atom to another, $r \equiv |\boldsymbol{r}|$. Let us consider a gas of dipoles in an external magnetic field that polarises them along the z axis, as shown in Fig. 1a.

In this case, potential (1) appears as

$$V_{\uparrow\uparrow}(\boldsymbol{r}) = d^2\frac{1-3\cos^2\theta}{r^3}. \quad (2)$$

The term with $\delta(\boldsymbol{r})$ is excluded because, due to the polarisation into a state with the same spins, the wave function of the

V.A. Vinogradov, K.A. Karpov, A.V. Turlapov Institute of Applied Physics, Russian Academy of Sciences, ul. Ulyanova 46, 603950 Nizhny Novgorod; International Centre for Quantum Optics and Quantum Technologies LLC, International Center for Quantum Technologies, Bol'shoi blv. 30/1, Skolkovo Innovation Center Area, 121205 Moscow, Russia; Moscow Institute of Physics and Technology (National Research University), Institutskii per. 9, 141701 Dolgoprudnyi, Moscow region, Russia;
e-mail: turlapov@appl.sci-nnov.ru;
M.V. Platonova Institute of Applied Physics, Russian Academy of Sciences, ul. Ulyanova 46, 603950 Nizhny Novgorod; International Centre for Quantum Optics and Quantum Technologies LLC, International Center for Quantum Technologies, Bol'shoi blv. 30/1, Skolkovo Innovation Center Area, 121205 Moscow, Russia; Lobachevsky University, prosp. Gagarina 23, 603950 Nizhny Novgorod, Russia

Received 14 March 2022; revision received 21 April 2022
Kvantovaya Elektronika **52** (6) 528–531 (2022)
Translated by M.A. Monastyrskiy

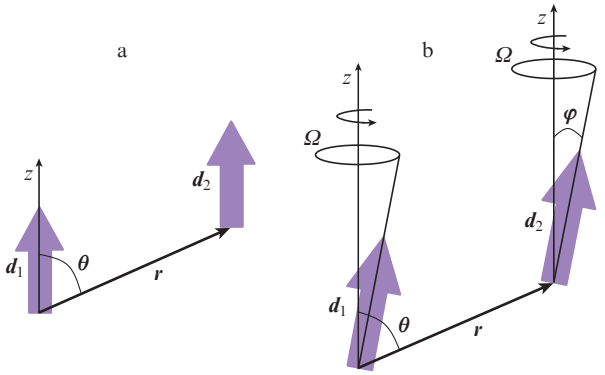

Figure 1. (a) Two magnetic dipoles polarised along the external magnetic field and (b) magnetic dipoles following the external magnetic field $\boldsymbol{B} \propto \boldsymbol{z}_0\cos\varphi + \sin\varphi[\boldsymbol{x}_0\cos(\Omega t) + \boldsymbol{y}_0\sin(\Omega t)]$, which rotates with the angular velocity Ω.

pair is antisymmetric, and, therefore, the expected value of the operator $\delta(\boldsymbol{r})$ for such a function is always zero. The anisotropy of the interaction is seen from formula (2): dipoles located one above the other ($\theta \approx 0$) attract, while dipoles located side by side ($\theta \approx \pi/2$) repulse.

A partial wave with an angular momentum l is exposed to the action of an effective potential composed of (2) and a centrifugal potential:

$$V_l(\boldsymbol{r}) = d^2\frac{1-3\cos^2\theta}{r^3} + \frac{\hbar^2 l(l+1)}{mr^2}, \qquad (3)$$

where m is the mass of the atom. Figure 2a shows the potential for a p-wave in the direction of greatest attraction. The dipole–dipole potential dominates the centrifugal one for $r < r_l \equiv 2d^2m/[\hbar^2 l(l+1)]$. For the p-wave, $r_{l=1} = 20$ nm. The atoms must approach each other to this distance, so that the p-interaction would not be shielded by a centrifugal barrier and the interaction energy would be noticeable against the kinetic energy background. For comparison, the p-interaction associated with the molecular potential, with the exception of resonant cases, requires converging by fractions of a nanometre. The interaction can be smoothly controlled, including changing the interaction sign. Let the magnetic field vector rotate, describing a cone around the z axis (see Fig. 1b). In this case, the rotation is slow enough for the dipoles to follow the field:

$$\boldsymbol{d}_1(t) = \boldsymbol{d}_2(t) = d\boldsymbol{z}_0\cos\varphi + d\sin\varphi[\boldsymbol{x}_0\cos(\Omega t) + \boldsymbol{y}_0\sin(\Omega t)]. \qquad (4)$$

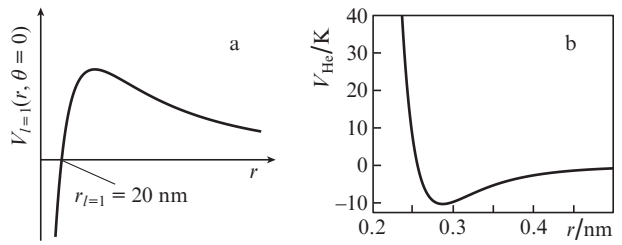

Figure 2. Interaction potentials of (a) two dysprosium atoms in the p-channel (3) in the direction of maximum attraction ($\theta = 0$) and (b) two ^{3}He atoms in the Lennard–Jones approximation [14].

When averaging over the rotation period, we obtain the effective potential [15]

$$\langle V(\boldsymbol{r},t)\rangle_t = d^2\frac{1-3\cos^2\theta}{r^3}\alpha(\varphi), \quad \alpha(\varphi) \equiv \frac{3\cos^2\varphi - 1}{2}. \qquad (5)$$

At $\varphi = \pi/2$, this potential becomes attractive for dipoles located side by side.

3. Superfluid phases in polarised dysprosium

Potential (2) is attractive for wave functions that are sufficiently elongated along the z axis, as can be seen from the matrix element

$$\langle l, l_z = 0\,|1 - 3\cos^2\theta\,|\,l, l_z = 0\rangle = -\frac{2l(l+1)}{4l(l+1)-3}, \qquad (6)$$

which is negative for all spherical harmonics $Y_{l0}(\theta)$, except for the harmonic with $l = 0$. The potential $V_{\uparrow\uparrow} \propto Y_{20}(\theta)$ ensures interaction between all partial waves with projection $l_z = 0$ and angular momenta l, $l \pm 2$. The attracting interaction allows the formation of Cooper pairs and a superfluid phase. Due to the antisymmetry of the pair state, only partial waves with odd l values participate in the pairing.

The critical phase transition temperature has been predicted in [16]:

$$T_{cr} = 1.44E_F\exp\left(-\frac{\pi E_F}{12nd^2}\right), \qquad (7)$$

where n is the gas concentration; and $E_F = \hbar^2(6\pi^2 n)^{2/3}/(2m)$. In the momentum space, the order parameter has an anisotropic dependence on the angle θ_p between the vectors $\boldsymbol{p}$ and $\boldsymbol{z}_0$:

$$\Delta \propto \cos\left(\frac{\pi}{2}\sin\theta_p\right), \qquad (8)$$

qualitatively repeating the angular dependence of the p-wave $Y_{10} \propto \cos\theta_p$, for which the dipole–dipole interaction yields the strongest coupling. Phases with the order parameter Δ close to $Y_{1,\pm1}$ can also be implemented. To this end, potential (5) can be used at $\varphi = \pi/2$.

4. Prospects for cooling dysprosium to the phase transition temperature

Dysprosium has two stable fermion isotopes, ^{161}Dy and ^{163}Dy, with a natural content of 18.9% and 24.9%, respectively. The ground state has the electronic configuration $[Xe]4f^{10}6s^2\,{}^5I_8$, and the nuclear spin of both isotopes is $I = 5/2$. For dysprosium, the exponent in formula (7) can be expressed in terms of the interparticle distance $n^{-1/3}$:

$$T_{cr} = 1.44E_F\exp\left(-\frac{n^{-1/3}}{10\text{ nm}}\right). \qquad (9)$$

Substituting, for example, $n^{-1/3} = 30$ nm into this expression, we find the critical temperature $T_{cr} = 0.07E_F$. A higher value of T_{cr}/E_F is unlikely, despite the significant pre-exponential factor in (9). The temperature T_{cr} is limited from above by $0.14E_F$, i.e. the Bose condensation temperature of point bosons with a mass of $2m$ and a concentration of $n/2$. Formula (7) is derived in the weak coupling approximation, $nd^2 \ll E_F$.

The temperature $T = 0.07E_F$ is on the verge of what can be obtained for Fermi gases. The ratio $T/E_F \approx 0.1$ is the lowest achieved, including for dysprosium [17]. The interparticle distance $n^{-1/3} = 30$ nm has not yet been obtained in experiments. Such a dense compression requires a sufficiently large number of N atoms. The characteristic size of the optical dipole trap is 10 μm or more. For a 10 μm trap, $N = 3 \times 10^7$ is required to reach $n^{-1/3} = 30$ nm. The prospect for obtaining $N = 3 \times 10^7$ particles at $T = 0.07E_F$ can be estimated by considering the gas preparation procedure. At the first stage, the gas of atoms is collected in a magneto-optical trap (MOT), which uses radiation with a wavelength of 626 nm. For ^{162}Dy bosons with a natural content of 25.5%, the largest number of atoms trapped in the MOT was 10^9 at a temperature of 6 μK [18]. In experiments where the trapping of fermion isotopes was studied, the number of atoms in the MOT (both bosons and fermions) was noticeably smaller. There is a general trend: the number of ^{161}Dy and ^{163}Dy fermions, respectively, is 6 and 1.2 times less than that of ^{162}Dy bosons [19, 20]. Further cooling to a temperature of quantum degeneracy was performed in an optical dipole trap. In [17], having started with a MOT containing $N = 2 \times 10^7$ ^{161}Dy particles, the authors obtained 4×10^4 atoms at a temperature of 60 nK, which corresponds to $T/E_F = 0.1$.

In order to obtain a significant number of particles in a state of degeneracy, it is possible to transfer most of the atoms from the MOT into a deep optical lattice [21] or a large dipole trap [22]. Further cooling in the dipole trap can be carried out with small particle losses provided inelastic processes are suppressed. For example, in work [23] quantum degeneracy was achieved at the cost of losing only 2/3 of all particles. An obstacle to increasing the gas density can be inelastic three-particle collisions, as a result of which two particles form a molecule, while the third one carries away the excess energy. Such collisions lead to gas heating and particle losses with an event frequency proportional to n^2. Similar collisions were observed in a Fermi gas with two spin components [24]. Compared to Bose gases, in Fermi gases, three-particle collisions are suppressed due to the Pauli exclusion principle, i.e. a low probability for three fermions, two of which are in the same internal state, to be in the range of the molecular potential. It is hoped that in a polarised dysprosium gas, three-body collisions will occur even less frequently. In the experiment with polarised ^{167}Er [25], the interparticle distance was brought to $n^{-1/3} = 140$ nm, and no inelastic collisions were observed. The potential complexity is also represented by the magnetic Fano–Feshbach resonances, which significantly increase the probability of inelastic collisions and are located quite close to each other, at least at a field strength of ~1 G [26].

Thus, obtaining $N = 3 \times 10^7$ dysprosium atoms at a temperature $T = 0.07E_F$ with an interparticle distance $n^{-1/3} = 30$ nm looks nontrivial and will require further development of laser cooling and trapping methods.

5. Comparison of dysprosium phases with ^{3}He phases

Cooper pairing in the p-channel and superfluid phases with the order parameter Δ having p-symmetry are implemented in the liquid ^{3}He. The interparticle interaction, in contrast to that in dysprosium, is spherically symmetric. The interaction potential in the Lennard–Jones approximation [14],

$$V_{He} \approx \frac{C_{12}}{r^{12}} - \frac{C_6}{r^6}, \tag{10}$$

is shown in Fig. 2b. It is repulsive near $r = 0$, and so pairing is only possible in states with a wave function 'moved away' from the centre. The strongest attracting interaction occurs in the p-channel, which makes the spatial wave function of the pair antisymmetric; therefore, the spin state must be symmetric in permutations with total spin $I = 1$. Nonzero values of the orbital and spin moments lead to a variety of possible phases. In general, the order parameter has the form

$$\Delta = \Delta_{I_z=1}(\boldsymbol{p})\uparrow\uparrow + \Delta_{I_z=0}(\boldsymbol{p})\frac{\uparrow\downarrow+\downarrow\uparrow}{\sqrt{2}} + \Delta_{I_z=-1}(\boldsymbol{p})\downarrow\downarrow, \tag{11}$$

where the arrows show the states of the nuclear spins in a pair. There are three possible projections of the total nuclear spin of the pair I_z, three projections of the orbital momentum l_z, and also a violation of gauge invariance.

Five superfluid phases have been implemented, for which the angular dependence of the order parameter $\Delta(\boldsymbol{p})$ in the momentum space and the spin composition are shown in Fig. 3. All three spin states participate in phase B [27, 28], which makes the order parameter spherically symmetric. Phases A [27,28] and A1 [28] have an order parameter with the spatial symmetry of the Y_{11} harmonic. The selection of spin and the appearance of the A1 phase require an external magnetic field. Phases A, A1, and B are implemented in homogeneous ^{3}He. When aerogel – thin filaments occupying a small percentage of the volume – is introduced into helium, the polar phase [29] and the polar β-phase [30] with the order parameter $\Delta \propto Y_{10}(\boldsymbol{p})$ in the basis with the z axis directed along the aerogel filament become energetically advantageous. Quasi-particles are scattered on the filament, which suppresses the motion across the filament and makes the motion of the pair along the filament more energetically advantageous.

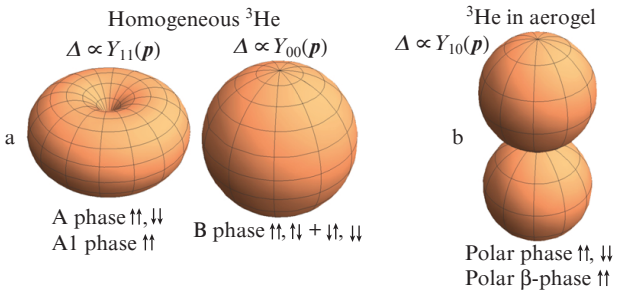

Figure 3. (Colour online) Superfluid phases of ^{3}He, (a) obtained in a homogeneous medium or (b) requiring the presence of aerogel filaments. The spin composition and the dependence $\Delta(\boldsymbol{p})$ of the order parameter on the momentum direction are shown.

The polar β-phase is closest to the hypothetical dysprosium phase in a constant magnetic field in terms of the shape of the order parameter and spin composition. The A1 phase is close to the dysprosium phase in a rotating field when interacting according to (5) with the parameter $\varphi = \pi/2$. However, in ^{3}He, the spin quantisation axis is perpendicular to the axis of orbital motion quantisation. For a dysprosium gas, these axes coincide.

Unlike the interaction in helium, the interaction in dysprosium is anisotropic. Thus, a phase state is possible in dysprosium, the macroscopic properties of which are entirely determined by the microscopic anisotropy. Anisotropy will manifest itself both in the ground state and in dynamic properties: according to the Landau criterion, the anisotropic excitation spectrum should give a dependence of the critical velocity on the angle, which repeats in shape the dependence of the order parameter on the angle.

The anisotropy of the interaction in Dy can be changed by using a rotating magnetic field and varying the angle φ of its inclination. This will allow tracking the response of macroscopic properties to changes in interaction.

Atomic gases are of interest for the observation of nonequilibrium processes and the kinetics of phase transitions due to the relatively low flow rate of these processes. The characteristic times are certainly longer than $\hbar/E_F = 300$ ns at $n^{-1/3} = 30$ nm. For dysprosium in a rotating magnetic field at $\varphi = \pi/2$, there is a degeneracy between phases with orbital angular momentum projections $l_z = \pm 1$. Thus, there should be a spontaneous choice between these two phases. It is of interest which processes will affect this choice and whether it will lead to a metastable supercooled state and to a shift in the phase transition temperature. For helium, there is no problem of such a choice, since in the A1 phase, the projection $l_z = 1$ is more advantageous due to the spin–orbit interaction.

The dysprosium gas in the trap is a closed system, and so the formation of a phase with the order parameter $\Delta \propto Y_{1,\pm 1}$ should be accompanied by the appearance of a vortex with opposite circulation. In helium, there is an exchange of angular momentum with the vessel walls, and therefore the angular momentum of the liquid is not preserved.

In the superfluid ^{3}He in the ground state, the Fermi surface is isotropic. In the excited state, its deformations occur, due to which the appearance of a superfluid flow is possible even in the case when the critical velocity is equal to zero in accordance with the Landau criterion [31]. In a polarised gas with dipole–dipole interaction, the Fermi surface is already deformed in the ground state [32]. It seems interesting to study the effect of deformation on the dynamics of the superfluid phase of dysprosium.

The description of the interaction in dysprosium is quite simple. This opens up the possibility of calculating collective properties entirely from first principles, similar to the calculations performed earlier for Fermi gases interacting through s-collisions. The experimental results can be used to test multiparticle computational methods.

6. Conclusions

The gas of dysprosium is a promising medium for producing superfluid phases with an anisotropic order parameter. It is assumed that the symmetry of the states will be determined by the symmetry of the interparticle interaction. The slow rate of the processes will allow us to study the kinetics of the superfluid phase formation.

Acknowledgements. The authors are greatfull to G.E. Volovik, V.V. Dmitriev, and M.Yu. Kagan for their helpful advice.

The work was supported by Rosatom State Corporation within the framework of the Quantum Technologies' Roadmap, the Russian Foundation for Basic Research (Grant Nos 19-29-11025 and 20-02-00015), and the Ministry of Education and Science (State Assignment of the Institute of Applied Physics of the Russian Academy of Sciences, No. 2021-0030-2021-0002).

References

1. Val'kov V.V., Dzebisashvili D.M., Korovushkin M.M., Barabanov A.F. *Phys. Usp*., **64**, 641 (2021) [*Usp. Fiz. Nauk*, **191**, 673 (2021)].
2. Vollhardt D., Wolfle P. *The Superfluid Phases of Helium 3* (London: Taylor & Francis, 1990).
3. Mizushima T., Tsutsumi Y., Kawakami T., Sato M., Ichioka M., Machida K. *J. Phys. Soc. Japan*, **85**, 022001 (2016).
4. Volovik G.E. *Topological Superfluids*; arXiv:1602.02595v6.
5. Gehm M.E., Hemmer S.L., Granade S.R., O'Hara K.M., Thomas J.E. *Phys. Rev. A*, **68**, 011401(R) (2003).
6. Ku M.J.H., Sommer A.T., Cheuk L.W., Zwierlein M.W. *Science*, **335**, 563 (2012).
7. Bartenstein M., Altmeyer A., Riedl S., Jochim S., Chin C., Denschlag J.H., Grimm R. *Phys. Rev. Lett*., **92**, 120401 (2004).
8. Kagan M.Yu., Turlapov A.V. *Phys. Usp*., **62**, 215 (2019) [*Usp. Fiz. Nauk*, **189**, 225 (2019)].
9. Bozovic I. *J. Supercond.*, **4**, 193 (1991).
10. Vinogradov V.A., Karpov K.A., Savelyeva S.V., Turlapov A.V. *Quantum Electron*., **49**, 433 (2019) [*Kvantovaya Elektron*., **49**, 433 (2019)].
11. Regal C.A., Ticknor C., Bohn J.L., Jin D.S. *Phys. Rev. Lett*., **90**, 053201 (2003).
12. Lu M., Burdick N.Q., Lev B.L. *Phys. Rev. Lett*., **108**, 215301 (2012).
13. Zangwill A. *Modern Electrodynamics* (Cambridge: Cambridge University Press, 2013).
14. Van Sciver S. *Helium Cryogenics. International Cryogenics Monograph Series* (New York: Springer, 2013).
15. Giovanazzi S., Gorlitz A., Pfau T. *Phys. Rev. Lett*., **89**, 130401 (2002).
16. Baranov M.A., Mar'enko M.S., Rychkov V.S., Shlyapnikov G.V. *Phys. Rev. A*, **66**, 013606 (2002).
17. Ravensbergen C., Corre V., Soave E., Kreyer M., Kirilov E., Grimm R. *Phys. Rev. A*, **98**, 063624 (2018).
18. Mühlbauer F., Petersen N., Baumgärtner C., Maske L., Windpassinger P. *Appl. Phys. B*, **124**, 120 (2018).
19. Youn S.H., Lu M., Ray U., Lev B.L. *Phys. Rev. A*, **82**, 043425 (2010).
20. Maier T., Kadau H., Schmitt M., Griesmaier A., Pfau T. *Opt. Lett*., **39**, 3138 (2014).
21. Kalganova E.S., Golovizin A.A., Shevnin D.O., Tregubov D.O., Khabarova K.Yu., Sorokin V.N., Kolachevsky N.N. *Quantum Electron*., **48**, 415 (2018) [*Kvantovaya Elektron*., **48**, 415 (2018)].
22. Vinogradov V.A., Karpov K.A., Lukashov S.S., Turlapov A.V. *Quantum Electron*., **50**, 520 (2020) [*Kvantovaya Elektron*., **50**, 520 (2020)].
23. Luo L., Clancy B., Joseph J., Kinast J., Turlapov A., Thomas J.E. *New J. Phys*., **8**, 213 (2006).
24. Du X., Zhang Y., Thomas J.E. *Phys. Rev. Lett*., **102**, 250402 (2009).
25. Aikawa K., Frisch A., Mark M., Baier S., Grimm R., Ferlaino F. *Phys. Rev. Lett*., **112**, 010404 (2014).
26. Baumann K., Burdick N.Q., Lu M., Lev B.L. *Phys. Rev. A*, **89**, 020701 (2014).
27. Osheroff D.D., Richardson R.C., Lee D.M. *Phys. Rev. Lett*., **28**, 885 (1972).
28. Lee D.M. *Rev. Mod. Phys*., **69**, 645 (1997).
29. Dmitriev V.V., Senin A.A., Soldatov A.A., Yudin A.N. *Phys. Rev. Lett*., **115**, 165304 (2015).
30. Dmitriev V.V., Kutuzov M.S., Soldatov A.A., Yudin A.N. *Phys. Rev. Lett*., **127**, 265301 (2021).
31. Autti S., Makinen J.T., Rysti J., Volovik G.E., Zavjalov V.V., Eltsov V.B. *Phys. Rev. Res*., **2**, 033013 (2020).
32. Aikawa K., Baier S., Frisch A., Mark M., Ravensbergen C., Ferlaino F. *Science*, **345**, 1484 (2014).